







Using Landsat images to monitor changes in the snow-covered area of selected glaciers in northern Pakistan


Chaman GUL^{1,2}  <http://orcid.org/0000-0001-6704-679X>; e-mail: chaman@lzb.ac.cn

KANG Shi-chang^{1,2,3*}  <http://orcid.org/0000-0003-2115-9005>;  e-mail: shichang.kang@lzb.ac.cn

Badar GHAURI⁴  <http://orcid.org/0000-0002-0709-9539>; e-mail: b_ghauri@yahoo.com

Mateeul HAQ⁵  <http://orcid.org/0000-0001-6867-6072>; e-mail: matee_haq@yahoo.com

Sher MUHAMMAD^{2,3}  <http://orcid.org/0000-0001-7315-6450>; e-mail: sher_muhammad84@yahoo.com

Shaukat ALI⁶  <http://orcid.org/0000-0001-7500-2121>; e-mail: pirshauki@gmail.com

* Corresponding author

¹ State Key Laboratory of Cryosphere Science, Northwest Institute of Eco-Environment and Resources, Chinese Academy of Sciences, Lanzhou 73000, China

² University of Chinese Academy of Sciences, No.19A Yuquan Road, Beijing 100049, China

³ CAS Center for Excellence in Tibetan Plateau Earth Sciences, Beijing 100101, China

⁴ Institute of Space Technology (IST), Karachi, Pakistan

⁵ Space and Upper Atmosphere Research Commission (SUPARCO), Karachi, Pakistan

⁶ Global Change Impact Studies Centre (GCISC), Ministry of Climate Change, Islamabad, Pakistan

Citation: Gul C, Kang SC, Ghauri B, et al. (2017) Using Landsat images to monitor changes in the snow-covered area of selected glaciers in northern Pakistan. *Journal of Mountain Science* 14(10). <https://doi.org/10.1007/s11629-016-4097-x>

© Science Press and Institute of Mountain Hazards and Environment, CAS and Springer-Verlag GmbH Germany 2017

Abstract: Landsat satellite images were used to map and monitor the snow-covered areas of four glaciers with different aspects (Passu: 36.473°N, 74.766°E; Momhil: 36.394°N, 75.085°E; Trivor: 36.249°N, 74.968°E; and Kunyang: 36.083°N, 75.288°E) in the upper Indus basin, northern Pakistan, from 1990–2014. The snow-covered areas of the selected glaciers were identified and classified using supervised and rule-based image analysis techniques in three different seasons. Accuracy assessment of the classified images indicated that the supervised classification technique performed slightly better than the rule-based technique. Snow-covered areas on the selected glaciers were generally reduced during the study period but at different rates. Glaciers reached maximum areal snow coverage in winter and pre-

monsoon seasons and minimum areal snow coverage in monsoon seasons, with the lowest snow-covered area occurring in August and September. The snow-covered area on Passu glacier decreased by 24.50%, 3.15% and 11.25% in the pre-monsoon, monsoon and post-monsoon seasons, respectively. Similarly, the other three glaciers showed notable decreases in snow-covered area during the pre- and post-monsoon seasons; however, no clear changes were observed during monsoon seasons. During pre-monsoon seasons, the eastward-facing glacier lost comparatively more snow-covered area than the westward-facing glacier. The average seasonal glacier surface temperature calculated from the Landsat thermal band showed negative correlations of -0.67, -0.89, -0.75 and -0.77 with the average seasonal snow-covered areas of the Passu, Momhil, Trivor and Kunyang glaciers, respectively, during pre-monsoon seasons. Similarly, the air temperature collected from

Received: 21 June 2016
Revised: 28 December 2016
Accepted: 05 June 2017

a nearby meteorological station showed an increasing trend, indicating that the snow-covered area reduction in the region was largely due to climate warming.

Keywords: Snow-covered area; Glacier; Global warming; Classification technique; Northern Pakistan

Introduction

The Himalayas–Karakoram–Hindu-Kush (HKH) region hosts multiple extended glaciers (Kääb et al. 2012). The Karakoram Range, situated in the upper Indus basin, has an extensive formation of glaciers due to its high altitude (Young et al. 1990). The eastern and northwestern Himalayas are seasonally snow covered; however, the snow-cover extent of the central Himalayas is relatively limited (Ménégoz et al. 2013b). Glaciers located in this region are an important source of freshwater for China, Pakistan, Nepal and India. Glaciers are also good indicators of climate change, and a minor climate variation, such as temperature change, can produce a rapid glacial response (IPCC 2013; Rabatel et al. 2013). The snow-covered area on a glacier affects water balance determination and radiation, which are important components in climate studies and the hydrological cycle (Stieglitz et al. 2001).

The extent, thickness and melt rate of snow-covered areas depend on geographical location, elevation, season, solar irradiance, and atmospheric pollutant concentrations and deposition on the snow surface (Kopacz et al. 2011; Ménégoz et al. 2014). In the Himalayas region, the largest snow extent occurs in the elevation zone between 3000 and 6000 m (Maskey et al. 2011). Glaciers in many parts of the world, such as those in the tropical Andes, are currently retreating, similar to those in Polar Regions (Bradley et al. 2006; IPCC 2013; Rabatel et al. 2013). Glacier shrinkage has also been prevailing over the Third Pole region (e.g., Kang et al. 2010; Kääb et al. 2012; Bolch et al. 2012; Neckel et al. 2014; Kang et al. 2015). Negative mass balance was also confirmed from in situ stake observations during the last decade for the Tibetan Plateau and Urumqi glacier no. 1 of the Tianshan Mountains (Zhang et al. 2014). Snow deposition and loss are primarily controlled by the atmospheric condition and state

of the land surface. Anthropogenic pollutants, such as black carbon deposited on snow, were found to shorten the snow cover season in the Northern Hemisphere (Ménégoz et al. 2013a). In the central Himalayas, it was estimated that the deposition of atmospheric pollution on snow could reduce the snow cover season at the rate of 8 days per year. It was also observed that depositions of black carbon on snow contribute significantly to the decrease in snow cover extent (Dery et al. 2007). Regional temperature variation, solar energy flux and precipitation are the main factors that affect a glacier's mass balance (Ribstein et al. 1998). It is expected that the present retreating behavior of glaciers will continue in the future (Oerlemans et al. 1998; Shi et al. 2000). Similarly, it has been found that both snow melt and snowfall were strongly influenced by even minor temperature increases (US EPA CCD Snow and Ice).

Satellite images are an important source of data for glaciological investigation and mapping, particularly in remote mountain regions (Rango et al. 1985). Freely available global Landsat data have been widely used for glacier snow-covered area mapping (Williams et al. 1997). Images of multi-spectral satellites, such as ASTER-Terra (Advanced Spaceborne Thermal Emission and Reflection Radiometer), Landsat TM (Thematic Mapper) and ETM+ (Enhanced TM Plus), HRV (High Resolution Visible), and SPOT (Satellite Pour l'Observation de la Terre), have been widely used for regional-scale change assessment and determination of glacier extent at a specific point in time (e.g., Paul et al. 2004; Racoviteanu et al. 2008; Bolch et al. 2010). In addition, time series satellite images have been used to determine snow-covered area and glacier extent at a specific point (Paul et al. 2004; Racoviteanu et al. 2008; Bolch et al. 2010). Freely available satellite data could be effectively used using an appropriate image classification technique to estimate precise glacier changes. There are many techniques available for separating various land covers (Rees et al. 2006). We select two frequently used techniques, namely, supervised and rule (or knowledge)-based image classification techniques (Muhammad et al. 2013). Both methods are useful and precise in terms of manual digitization (Paul et al. 2013), but supervised-based classification provides more consistent results and is useful for small-scale

studies (Muhammad et al. 2013).

Surface air temperature and precipitation are two important meteorological parameters for snow-covered area reduction in the region. Heavy rainfall occurred in the study region during summer monsoon seasons (Mooley et al. 1987). Monsoon precipitation amplified rainfall events due to the influence of topography (Barros et al. 2006). The distribution of ground precipitation was influenced by the size and shape of the mountains in the region. The thermodynamic effect was also a contributing factor of the heavy precipitation events in northern Pakistan (Lau et al. 2012). During the last century, the northwestern Himalayan region warmed at a significantly higher rate than the global average (Bhutiyan et al. 2007).

In this study, four glaciers of different aspects located in the Hunza basin of the upper Indus river basin were selected to investigate snow-covered area changes in different seasons from 1990-2014. A suitable classification method for snow-covered area mapping was identified. The snow-covered area was identified and separated using the supervised classification technique. The aim of this work was to understand the changes in snow-covered area on four selected glaciers in the Karakoram region and relate these changes to changes in climate for the period 1990-2014.

1 Study Region and Datasets

High mountain ranges, including the Himalayas, Karakoram and Hindu-Kush, are located in northern Pakistan and host numerous glaciers. According to the estimation of the International Centre for Integrated Mountain Development (ICIMOD), there are 5218 glaciers located in northern Pakistan. This study analyzed the seasonal snow-covered area on four glaciers (Passu, Momhil, Trivor and Kunyang), as shown in

Table 1. The selected glaciers are located in the Karakoram Range in the upper Indus basin of the Hunza valley, northern Pakistan (Figure 1). The glaciers outlines were extracted by classification method and not extracted by existing glacier outlines, that were further modified using Global Positioning System (GPS) data collected in the field. Further, with the help of Digital Elevation Model (DEM) and Google Earth, the glaciers outlines were improved. One objective of the study was to determine the role of glacier aspect in snow-covered area reduction. These four glaciers have aspects in four different directions, and the authors were familiar with in situ observations of glaciers located in this region with respect to the climatic conditions and snow-covered area fluctuations; therefore, these four glaciers were selected for the analysis. The total area of selected glaciers was approximately 300 km².

Landsat TM and ETM+ (Enhanced TM Plus) images were used for snow-cover mapping during 1990-2014. After May 2003, there was a scan line problem with ETM+ images, preventing their use for image analysis. Therefore, data before May 2003 were used from this sensor. During 1990 and 1991, no cloud-free satellite image was available for the study region. Most of the images were covered by clouds, especially during winter; however, only cloud-free images were used excluding the winter season that could make the results uncertain for this study. A total of 99 Landsat images (49 images from 1990 to 2003 and 50 images from 2011 to 2014) were downloaded and processed for snow-covered area calculation. All the acquired images were divided between two periods (early and late) and among three seasons, namely, pre-monsoon (April to June), monsoon (July to September) and post-monsoon (October to December). Images acquired from 1990-2003 were in the early period, and images acquired from 2011-2014 were in the late period. The pre-monsoon and monsoon

Table 1 Attributes of selected glaciers in northern Pakistan.

Glacier	Landsat image Path/row	Location	Aspect	Area (km ²)	Elevation (m a.s.l.)* max/min/mean
Passu	149/035	36.473°N 74.766°E	East	96±3	7286/2716/5112
Momhil	149/035	36.394°N 75.085°E	North	51	7178/3049/4955
Trivor	149/035	36.249°N 74.968°E	West	53	7145/3532/5196
Kunyang	149/035	36.083°N 75.288°E	South	93	7703/3078/472

Note: * Maximum, minimum and mean elevation of glaciers were taken from a glacier inventory of the Himalayas region.

seasons had more cloud-free images than the post-monsoon seasons. Totals of 49 and 50 cloud-free images were processed for the early and late period, respectively, as shown in Table 2. Meteorological stations around the study area were sparse. Daily temperature and precipitation data of the past 32 years were collected from a meteorological station (Gilgit pilot balloon observatory, 35°55' N, 74°20' E, 1460 m a.s.l.) located in the Gilgit region of northern Pakistan. There were three meteorological stations in the surrounding regions of the study area, namely, Naltar (36.29°N, 74.12°E, 2858 m a.s.l.), Ziarat (36.73°N, 74.62°, 3669 m a.s.l.), and Khunjerab (36.83°N, 75.40°E, 4730 m a.s.l.), operated by the Pakistan Water and Power Development Authority (WAPDA). Data from these three stations were limited, and therefore, precipitation and temperature data of the Gilgit

observatory were used. Significant correlations were found for mean, minimum and maximum temperature trends among the three stations of the Hunza basin and Gilgit station (Tahir et al. 2011). Before 1960, there were large gaps in the data (Sheikh et al. 2009); hence, only data after 1980 were used in this study. The temperature data collected from the Landsat thermal band were also used. Digital Number (DN) values of the sensor were converted into radiance values specific to the individual scene, and then the radiance values were converted into temperature by using the following formula:

$$T = \frac{K2}{\ln\left(\frac{K1}{L\lambda} + 1\right)}$$

where T is the temperature in Kelvin, $K1$ and $K2$ are the band-specific thermal conversion constants and $L\lambda$ is the top of atmosphere spectral radiance.

2 Methods

2.1 Image classification

Five basic steps (data acquisition, pre-processing, image classification, accuracy assessment of classified image and snow-covered area calculation) were applied for extracting and calculating snow-covered areas. After the acquisition of Landsat images, some initial processing (pre-processing), such as layer stacking, atmospheric correction (convert digital numbers to radiance and then convert radiance to reflectance) and sub-setting on each of the Landsat scenes, was performed (Liang et al. 2001). The acquired images were stacked as single layers. The DN values of the images were converted into radiance values and then atmospherically corrected to remove atmospheric effects.

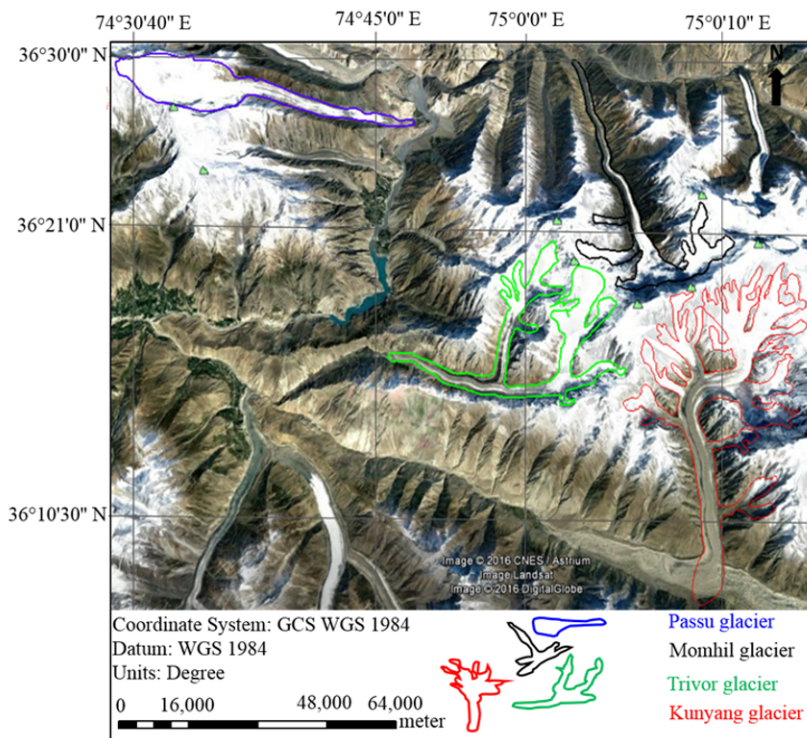


Figure 1 Study area map of the selected four glaciers.

Table 2 Number of images downloaded for each selected glacier during the study period

Season	Early period (1990 to 2003)				Late period (2011 to 2014)			
	Passu	Momhil	Trivor	Kunyang	Passu	Momhil	Trivor	Kunyang
Winter	0	1	0	0	1	1	0	1
Pre-monsoon	5	5	5	5	5	5	5	5
Monsoon	4	4	4	4	4	4	4	3
Post-monsoon	3	3	3	3	3	3	3	3

During the sub-setting process, individual glaciers were extracted from the Landsat scene through their shapefiles. To classify snow-covered areas from soil and rocks, supervised classification and knowledge-based techniques were used. In supervised classification, spectral signatures of snow were developed from specified locations on the image. These specified locations were given the generic name 'training sites'. This procedure was conducted using a vector layer containing training polygons. Training samples were selected by visual interpretation in the false-color composite displayed images and used as an input with the maximum likelihood classifier for extraction of debris-covered and snow-covered areas. The spectral signatures of snow and rocks/mud taken on Kunyang glacier are shown in Figure 2.

Selection of training polygons, creation of signature files for snow-covered areas and classification were the three basic steps of supervised classification. First, multiple polygons of various sizes were created for snow-covered areas to ensure that the software had sufficient information for creating spectral signatures. These signatures were used by the computer software to classify the selected images for snow-covered areas. In contrast, the knowledge-based or ruled-based method classified the images based on spectral ranges and predefined rules. The ranges were

selected in visible and near infrared bands because snow is highly reflective in the visible part and highly absorptive in the near infrared or shortwave infrared part of the spectrum. In addition to the above criteria, Normalized Difference Snow Indices (NDSIs) were used as input to the knowledge-based classification method to map the snow-covered areas. Depending on snow age and season, the NDSI threshold value used for snow ranged between 0.4 and 0.55.

$$NDSI = \frac{\text{Visible} - \text{Near Infrared}}{\text{Visible} + \text{Near Infrared}}$$

Previously, NDSI has been used for snow-covered mapping through various sensors (Dankers et al. 2004; Sirguey et al. 2008; Nagler et al. 2008). Each classified image was analyzed in terms of accuracy; if an image had erroneous output, then the classification process was repeated again. Misclassified areas of the image were manually edited. Although digitization and manual editing of classified images are time consuming, this method is the most accurate for glacier mapping (Albert et al. 2002). The results of the two classification techniques were assessed in terms of accuracy (Section 2.2). Snow-covered areas were identified through supervised classification, and output maps were generated. The methodology flowchart is shown in Figure 3.

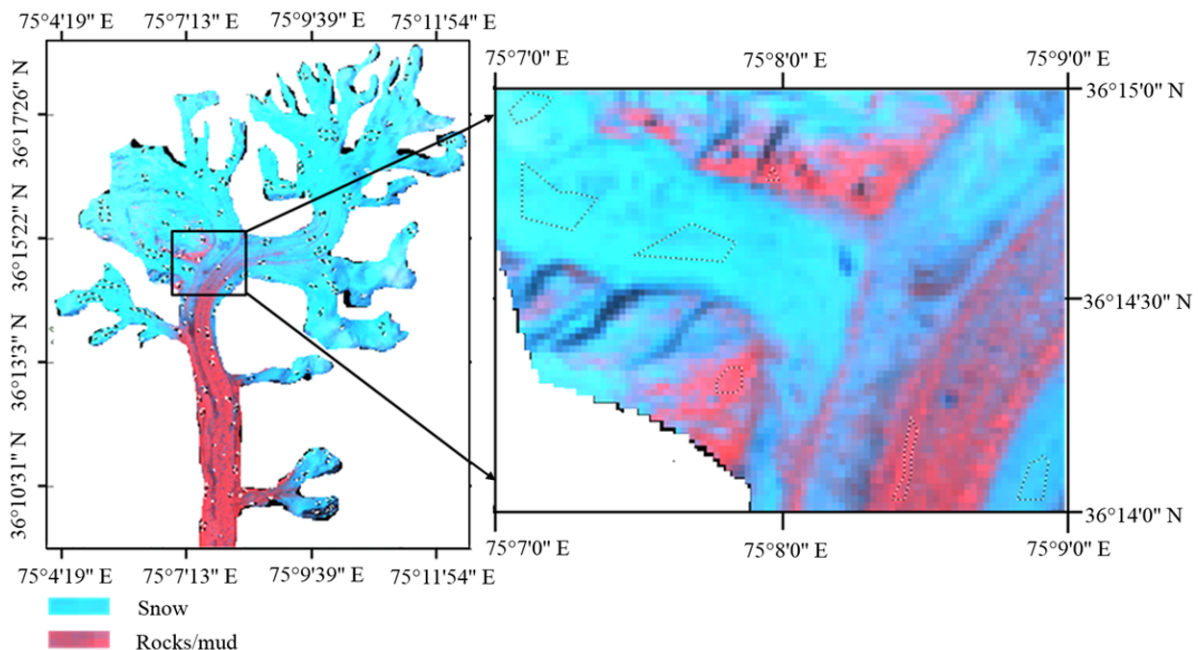


Figure 2 Training polygons and signatures of snow and rocks on Kunyang glacier (dotted line on right side indicate signatures).

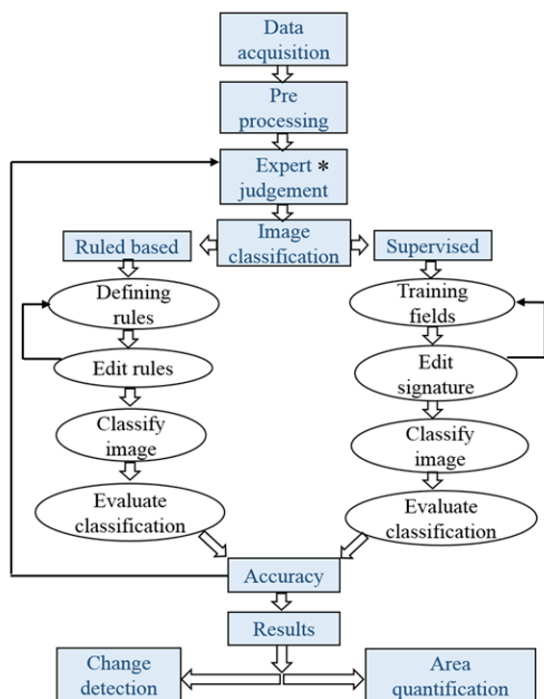


Figure 3 Methodology flow chart of satellite image acquisition, processing steps and image classification accuracy. (* Each classified image was analyzed in terms of accuracy; if an image had erroneous output, then the classification process was repeated.)

Table 3 Evaluation of the supervised classification based on an error matrix

Classified data	Reference data			Row total	Correctly classified
	Snow	Debris	Water		
Snow	142	12	6	160	88.7%
Debris	2	148	10	160	92.5%
Water	6	3	151	160	94.3%
Column total	150	163	167	480	

2.2 Accuracy assessment

The accuracy assessments reflect the difference between the classified image and the reference image. The accuracy of the classification was assessed by comparing the classified image with the reference image, which reflected the true land cover. Our interpreted image made with the help of ground truth information, higher-resolution satellite images, and maps derived from aerial photography was used as the reference image. Separate reference images (reference and classified images were from the same season) were used for each season. Manual editing after classification reduced the mismatch and increased the accuracy. It was not practical to test every pixel in the

classified image; therefore, representative samples of points of known class values (snow sample points) were used for the comparison. Forty reference points per glacier (160 reference points for four glaciers) were randomly selected from the reference image and then compared with the classified image. The data points were selected randomly using ENVI software, and no human bias was involved in the process. A table in the form of an error matrix was generated by comparison of the selected pixels in a classified and reference image. Rows and columns of the matrix contain pixels that permit the calculation of the overall accuracy of the classification. Agreement and disagreement were summarized in the cells of the error matrix during the comparison. The overall accuracy of the classified map was determined by dividing the total correct pixels (sum of the major diagonal) by the total number of pixels in the error matrix (N), as shown in Table 3. Supervised classification was relatively more effective than knowledge-based classification in detecting glacier changes, with 92% and 85% overall accuracy, respectively. Therefore, the snow-covered areas of all glaciers were calculated by using the supervised classification technique.

3 Results and Discussion

3.1 Snow-covered area changes on selected glaciers

Averaged seasonal snow-covered areas on selected glaciers during early and late periods are shown in Figure 4. Cloud-free images were limited especially during the winter season therefore, to avoid uncertainty in the results we removed the limited cloud free winter data. Information on the acquired images during late and early periods is provided in Table 4. Cloudy conditions inhibit incoming short wave radiation, whereas increased albedo due to fresh snowfall results in less energy available for snow melt (Archer et al. 2003). The maximum snow-covered area was found during the pre-monsoon seasons; however, the minimum snow-covered area was observed in the monsoon season. Precipitation in the form of snow during the pre-monsoon seasons, and snow starts melting quickly in the monsoon season due to the higher

temperature and the precipitation difference between the pre-monsoon and monsoon seasons. The snow-covered areas in the monsoon season are generally found at altitudes greater than 3000 m (Maskey et al. 2011). The average snow-covered area in the early period of the monsoon season was approximately 61.2, 31.8, 37.9 and 52.7 km² on the Passu, Momhil, Trivor and Kunyang glaciers, respectively. The average snow-covered area in the late period of the monsoon was almost the same as in the early period of the monsoon. The minimal snow-covered area during the early and late periods of the monsoon season may be due to the relatively high temperature and clear sky during this season. Based on the total area occupied by each glacier, the largest snow-covered area was observed on Passu glacier and the smallest was on Momhil glacier (Figure 4).

3.1.1 Intra seasonal and period wise snow-covered area changes

The maximum intra-seasonal snow-covered area change was observed on the Kunyang glacier, i.e., a reduction from 27.9 km² to 13.8 km² from the pre-monsoon to monsoon season of the early and late periods, respectively. During the monsoon to post-monsoon season, the Kunyang glacier gained 17.4 km² in snow-covered area in the early period and 6.8 km² in snow-covered area during the late period. Similarly, the minimal intra-seasonal snow-covered area change observed in the

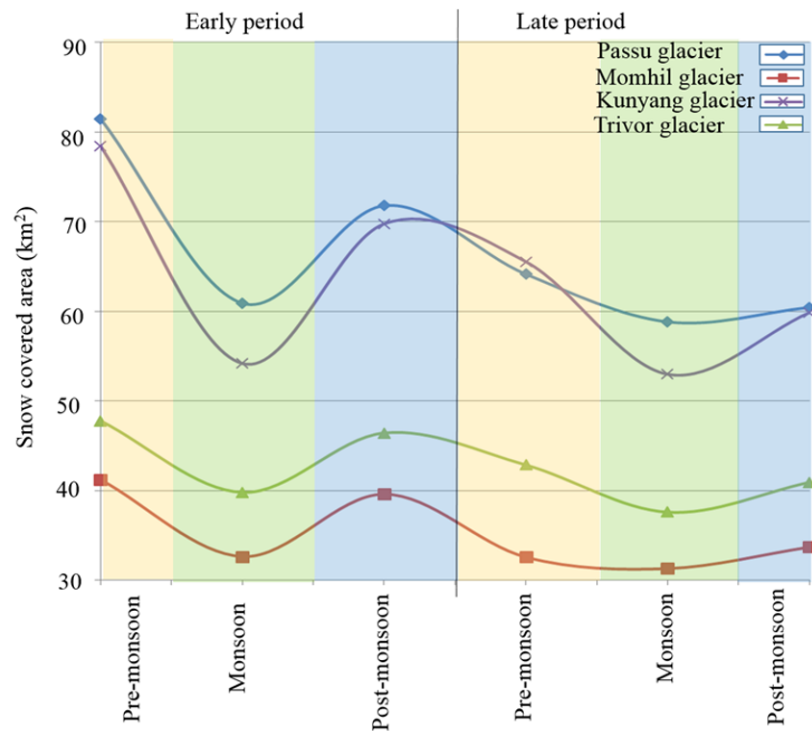


Figure 4 Seasonal comparison of snow-covered area for selected glaciers during early (1990-2003) and late periods (2011-2014).

Table 4 Information of the images acquired during late and early periods

Season	Period	Date	Subset glaciers
Winter	Early	5 th Feb 1999	Momhil
	Late	29 th Jan 2014	Passu, Mumhil and Trivor
Pre-monsoon	Early	10 th April 2002	Passu, Momhil, Trivor and Kunyang
		13 th April 2003	Passu, Momhil, Trivor and Kunyang
		26 th Apr 1999	Passu, Momhil, Trivor and Kunyang
		29 th Apr 2003	Passu, Momhil, Trivor and Kunyang
	Late	9 th May 1999	Passu, Momhil, Trivor and Kunyang
		27 th April 2011	Passu, Momhil, Trivor and Kunyang
		2 nd May 2013	Passu, Momhil, Trivor and Kunyang
		18 th May 2013	Passu, Momhil, Trivor and Kunyang
Monsoon	Early	23 rd Jul 1999	Passu, Momhil, Trivor and Kunyang
		13 th Aug 1998	Passu, Momhil, Trivor and Kunyang
		16 th Aug 1999	Passu, Momhil, Trivor and Kunyang
		16 th Aug 2002	Passu, Momhil, Trivor and Kunyang
	Late	21 st Jul 2013	Passu, Momhil, Trivor and Kunyang
Post-monsoon	Early	24 th July 2014	Passu, Momhil, Trivor and Kunyang
		17 th Aug 2011	Passu, Momhil and Trivor
		7 th Sep 2013	Passu, Momhil, Trivor and Kunyang
Post-monsoon	Early	03 rd Oct 2002	Passu, Momhil, Trivor and Kunyang
		1 st Nov 1998	Passu, Momhil, Trivor and Kunyang
	Late	19 th Nov 1998	Passu, Momhil, Trivor and Kunyang
		09 th Oct 2013	Passu, Momhil, Trivor and Kunyang
		25 th Oct 2013	Passu, Momhil, Trivor and Kunyang
		26 th Nov 2013	Passu, Momhil, Trivor and Kunyang

Table 5 Snow covered area (km²) on selected glaciers during three seasons (***** = image not available)

Season	Date	Passu glacier	Momhil glacier	Trivor glacier	Kunyang glacier
Pre-monsoon	May-1998	81.831	40.807	41.611	76.619
	Apr-1999	81.677	40.807	51.856	82.855
	Apr-2003	80.859	41.728	49.807	75.809
	May-2011	61.981	33.049	39.993	61.882
	May-2013	67.563	31.894	43.912	68.724
	Jun-2014	62.843	32.735	44.617	65.948
Monsoon	Aug-1998	57.080	29.705	37.004	51.989
	Oct-1998	*****	38.288	46.790	56.017
	Aug-1999	59.859	31.506	36.699	53.388
	Sep-2000	65.420	*****	*****	*****
	Sep-2001	63.760	*****	*****	*****
	Aug-2002	58.316	31.005	38.657	55.261
	Aug-2011	58.230	33.591	39.231	*****
	Sep-2013	59.088	29.843	36.424	52.724
	Jul-2014	59.103	30.147	37.062	53.197
	Post-monsoon	Oct-1992	76.444	*****	*****
Oct-1998		68.720	*****	*****	*****
Nov-2002		70.171	39.585	46.414	69.748
Oct-2013		60.427	33.677	40.906	59.843

Momhil glacier may be the result of less occupied area compared to the other three glaciers. There was more snow area change in the early period than in the late period. The early period was long (1990 to 2003) compared to the late period (2011 to 2014), as shown in Table 2. An abrupt decrease and increase of snow-covered areas were observed during the early period. Comparatively smooth changing behavior was observed during the late period.

3.1.2 Time series plots of snow-covered area

A time-series of snow-covered area in different seasons of the Passu glacier is shown in the third column of Table 5. The average snow-covered area during the pre-monsoon season was approximately 82.42 km² and 62.25 km² for the early and late periods, respectively.

The average snow-covered area for the Passu glacier in the monsoon season was approximately 61 km². No apparent change in snow-covered area was observed during the monsoon season. In the post-monsoon season, the snow-covered area of the Passu glacier was reduced by approximately 11.25%.

A time-series of snow-covered area changes in different seasons of the Momhil glacier is shown in the fourth column of Table 5. The total snow-covered area of the Momhil glacier was less than that of the Passu glacier; however, a similar trend in snow-covered area changes was observed

between these two glaciers. Similar trends in snow-covered area changes were also observed in the remaining two glaciers, Trivor and Kunyang, during the study period.

3.1.3 Snow-covered area mapping

Snow-covered area maps for the selected glaciers in the pre-monsoon season are shown in Figure 5. During the snow-covered mapping process, images of the same months were selected from the late and early periods. Visual observations and mathematical analysis indicated a clear reduction in snow area from the early to late period during the pre-monsoon season. The reduction in snow area was more visible at the terminus of each glacier. In the case of Passu glacier, the early period snow-covered area was 82.42 km² and late period snow-covered area was 62.25 km², indicating a 24.50% loss during the study period. Similarly, the area lost for the Momhil, Trivor and Kunyang glaciers was 21.4%, 10.2% and 16.4%, respectively (Figure 4 and Figure 5).

3.2 Seasonal averaged snow-covered area reduction

The average snow-covered area differences between the early and late periods are plotted and shown in Figure 6. The smallest snow cover changes were observed during the monsoon season, and larger changes were observed during the pre-

monsoon season. In the case of Passu glacier, the snow-covered area reduction was approximately 24 km², 11 km² and 3 km² for the pre-monsoon, post-monsoon and monsoon seasons, respectively. After Passu glacier, Momhil glacier (facing north) lost the second largest snow-covered area, i.e.,

approximately 21.8 km², 14.75 km² and 3.4 km² in the pre-monsoon, post-monsoon and monsoon seasons, respectively. A similar snow-covered area reduction trend was also observed on the remaining two glaciers, Trivor and Kunyang. This snow area reduction behavior may be due to increasing temperatures in the pre-monsoon season and decreasing temperatures in the monsoon season in the region (temperature trends are shown in Figure 7 and Figure 8). During the post-monsoon season, the snow-covered area lost by the selected glaciers was almost the same, i.e., approximately 12.25 ± 1 km². Kunyang glacier during the monsoon season showed slight increases in snow-covered area.

During the pre- and post-monsoon seasons, there was a clear snow cover reduction on selected glaciers, but in the monsoon season, the snow area was slightly reduced for three glaciers, namely, Passu, Momhil and Trivor; however, the snow area for Kunyang glacier was slightly increased.

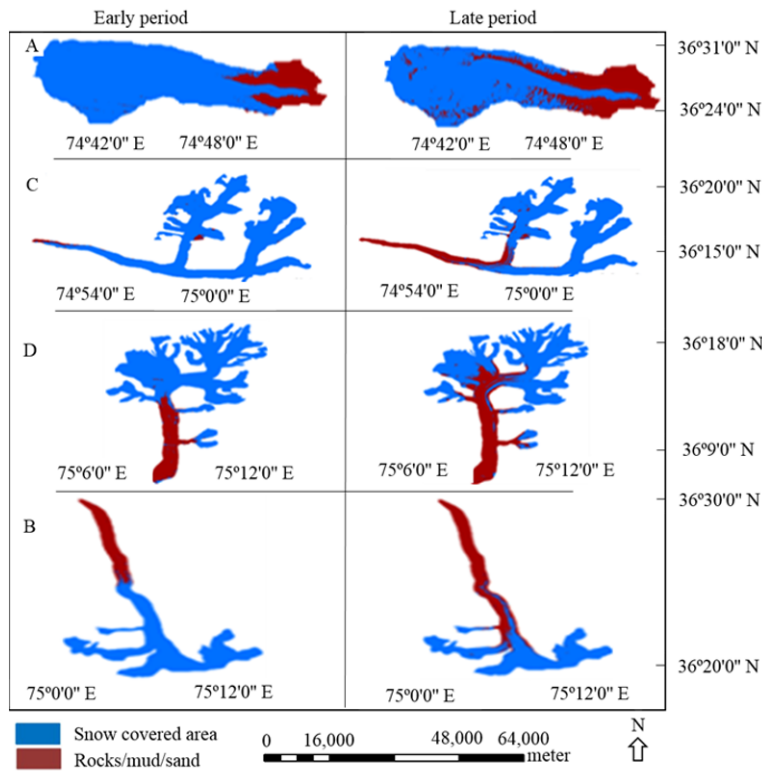


Figure 5 Snow-covered area maps during early (1990-2003) and late (2011-2014) periods of the pre-monsoon season (A = Passu, B = Momhil, C = Trivor and D = Kunyang).

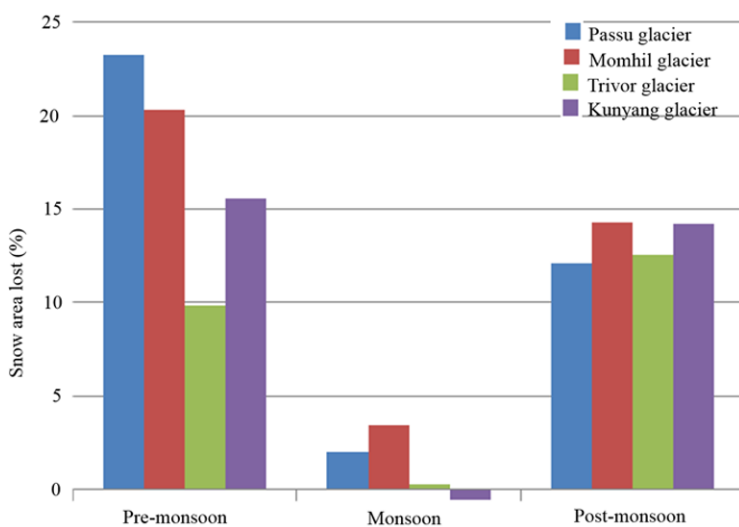


Figure 6 Snow-covered area lost, during the study period in the three seasons (slight gain on Kunyang glacier during the monsoon season).

3.3 Impact of glacier aspect

The slope and aspect can change the incoming shortwave radiation with respect to changes in the zenith angle. It was a common observation that snowfall reached a maximum at a particular glacier aspect depending on the wind direction at the time of snowfall. The glaciers also have very different morphologies. Different surrounding topographies likely have large impacts on the volume of accumulated snow, the duration for which the surface is in direct sunlight, and other factors. Therefore, these factors should be considered because they lead to quite different environmental conditions. Geographically, these glaciers are located close to each other (Figure 1), and it was assumed that they were exposed to almost the same

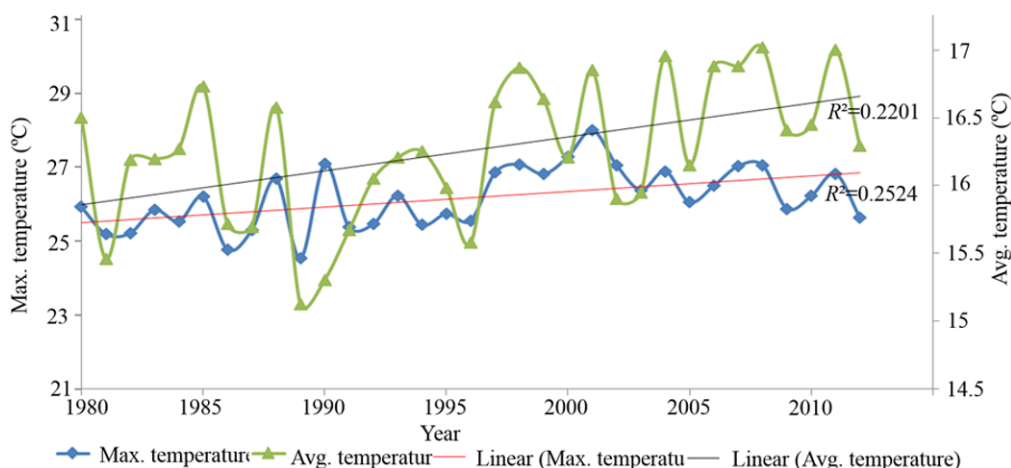


Figure 7 Annual averages of daily maximum temperature and daily average temperature.

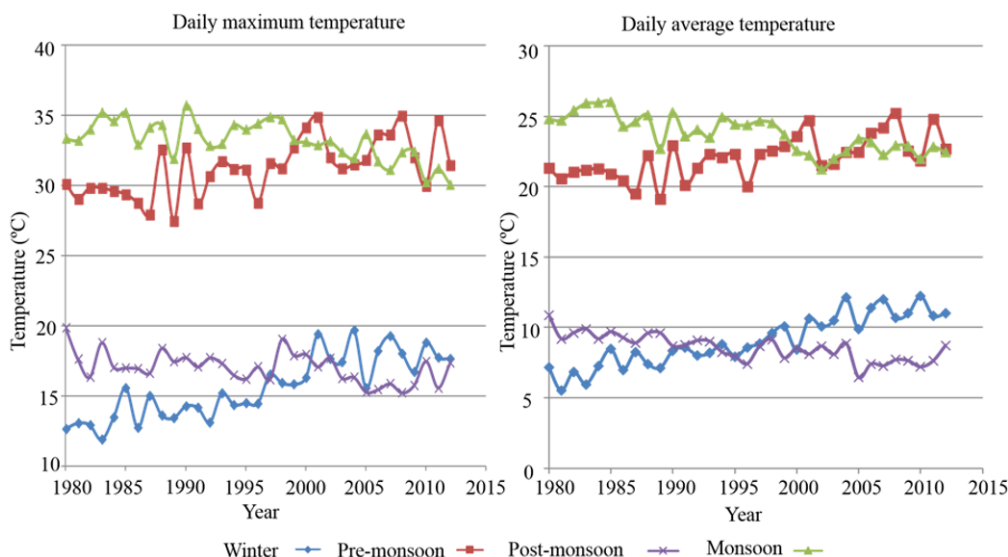


Figure 8 Seasonal averages of daily maximum temperature and daily average temperature near the study region.

environmental conditions. The only difference was the aspect of each glacier, which was the primary cause of the different melting rates during the same seasons. According to Young et al. 1990, the direction of annual precipitation was from the northwest, which may affect the glaciers facing east and south more than those facing north and west.

3.4 Seasonal impact

In the pre-monsoon season, the glacier facing east (“Passu”) lost the largest snow-covered area, whereas Trivor glacier, facing west, lost the least area of snow cover during the study period. This effect may be due to the maximum solar flux on glaciers facing east versus those facing west.

Momhil and Trivor glaciers had approximately the same area (Table 1); however, due to differences in their aspect, they exhibited differences in snow area reduction in the same season (Figure 6). For example, Momhil glacier showed a greater reduction in snow-covered area in the pre-monsoon season than in the post-monsoon season; however, Trivor glacier lost more snow area in the post-monsoon season than in the pre-monsoon season (Figure 6). Similarly, in the monsoon season, Momhil glacier experienced maximum reduction and Trivor glacier experienced minimum reduction in snow-covered area, whereas on Kunyang glacier, snow-covered area increased. Intra-seasonal snow-covered area variation rates were the greatest for Kunyang glacier and least for

Momhil glacier (Figure 4).

3.5 Temperature trend

Various model-based results indicate an increasing temperatures trends in the region (Ali et al. 2015). IPCC (2007) also reported that rainfall and temperature were likely to increase along with river flow in this region. These climatic changes may have caused the higher rate of snow melt. The possible reasons for the increasing snow melt in the region may be temperature and precipitation in the future (Ali et al. 2015). Similarly an increasing trend in pre-monsoon temperature may cause a decrease in snow-covered area in this season. Archer et al. (2003) found that summer runoff in this region was highly correlated with the summer mean temperature, which was an indication of the high snow melt in this season. Furthermore, it was reported that a 1°C increase in average summer temperature can result in a 15% to 16% increase in summer runoff (Archer et al. 2003).

3.5.1 Annual temperature

The annual average of daily maximum and daily average temperatures calculated from the Pakistan Meteorological Department (PMD) is shown in Figure 7. The light green line shows the annual average of daily temperature and the blue line shows the annual average of daily maximum temperature in the Gilgit region of northern Pakistan. The R^2 values for annual averages of maximum daily temperatures and annual averages of daily temperatures were 0.252 and 0.220, respectively (Figure 7). Although temperature was not highly correlated with time, visual interpretation suggests an increasing trend both in annual average daily maximum temperatures and daily average temperatures.

3.5.2 Seasonal temperature

The snow-covered area on selected glaciers was correlated with the air temperature data. The Pearson correlation between average seasonal temperature and average seasonal snow-covered area showed negative correlations of -0.78, -0.66, -0.39, and -0.65 for Passu, Momhil, Trivor and Kunyang glaciers, respectively, indicating that snow-covered area was decreasing with increasing temperature during the pre-monsoon season. A

similar negative correlation was observed for the Passu and Momhil glaciers during the monsoon season. Seasonal snow cover data during the post-monsoon was too limited for correlation analysis. Seasonal averages of daily maximum temperature and daily average temperature were calculated for three seasons for the period 1980-2013 (Figure 8).

The R^2 values for seasonal averages of daily average temperatures showed high correlation with time. In the case of daily average temperatures, the R^2 values for the winter, pre-monsoon, monsoon and post-monsoon seasons were 0.84, 0.44, 0.62 and 0.61, respectively. An increasing trend was observed in average daily maximum temperature and daily temperature during the winter and pre-monsoon seasons; however, there was a decreasing trend during the monsoon season.

The decreasing trend of temperature during the monsoon season does not support the snow-covered area increase in the study area, as is shown in the winter season. This discrepancy suggests that other meteorological parameters, such as precipitation and the concentration of pollutants deposited on the snow surface, play an important roles in the dynamics of snow-covered area.

3.5.3 Landsat based glacier surface temperature

Seasonal averages of glacier surface temperature collected from the Landsat satellite during pre-monsoon, monsoon and post-monsoon seasons of the early and late period are shown in Figure 9. Glacier surface temperature was calculated from the same image from which snow-covered area was calculated. An increasing trend in glacier surface temperature was observed from the early to late period. The correlations between this average seasonal temperature and average seasonal snow-covered area during the early and late periods were -0.67, -0.89, -0.75 and -0.77 for Passu, Momhil, Trivor and Kunyang glaciers, respectively, which was clear evidence that the snow-covered area in the region was decreasing with increasing temperature.

Glacier surface temperature variation on Momhil glacier during 1990-2003 and 2011-2014 is shown in Figure 10. The temperature was higher at the terminus than in the upper portions of the glaciers. The debris-covered area near the terminus absorbs solar radiation, whereas in the high-

elevation zones, fresh snowfall increases the albedo.

3.6 Precipitation trend

The maximum snow-covered area (approximately 80%) was observed in the winter and early pre-monsoon seasons; however, this snow-covered area decreases (up to 30%) in summer (Tahir et al. 2011). Annual precipitation in the upper Indus basin was mainly concentrated in the spring and winter and originated from the west (Young et al. 1990). Figure 11 shows the seasonal average daily precipitation in the Gilgit region. The mean annual precipitation at Gilgit station was approximately 0.412 ± 2 mm during the period 1980-2013. There was no significant correlation between the precipitation and snow-covered area change. R^2 values were less than zero in all seasons of the year. The Pearson correlations between average seasonal precipitation and average seasonal snow-covered area showed a weak positive relationship, with values of 0.46, 0.47, 0.18 for Passu, Momhil and Kunyang glaciers, respectively, indicating that snow-covered area may be increasing with increasing precipitation during the pre-monsoon season. A similar positive relationship was observed for Passu and Momhil glaciers during the monsoon season. One possible reason for this weak

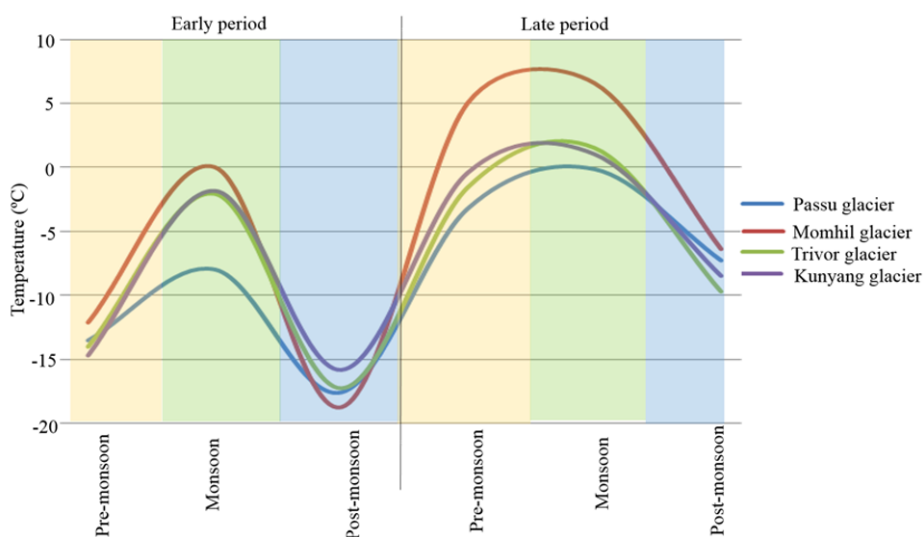


Figure 9 Seasonal average glacier surface temperatures during early (1990-2003) and late (2011-2014) periods.

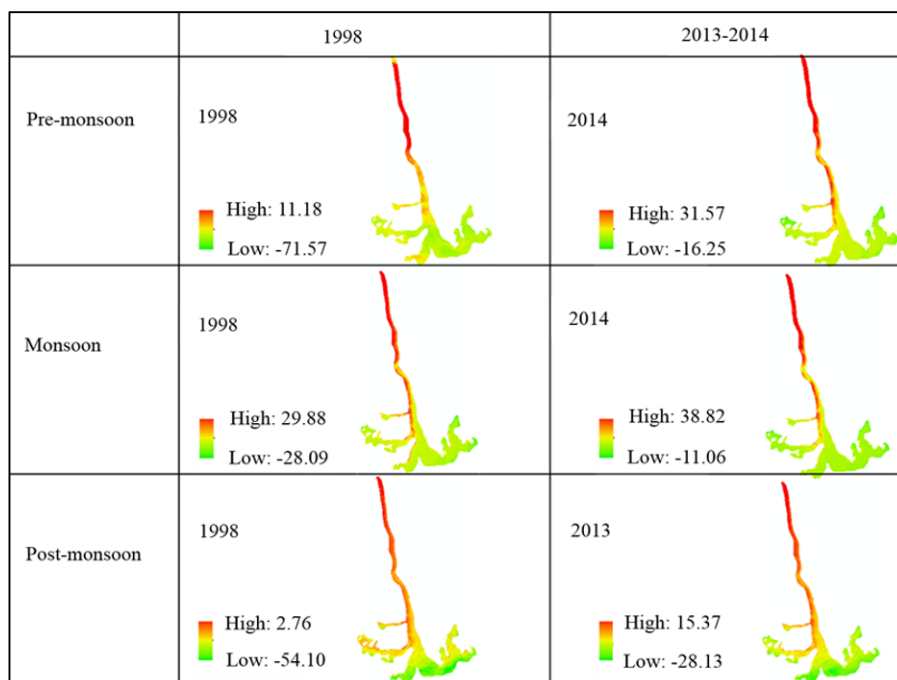


Figure 10 Surface temperature variation of Momhil glacier, extracted from Landsate satellite.

correlation may be the altitude difference among the locations of precipitation observation stations and the selected glaciers. The stations are located at lower elevations, whereas the snow-covered areas were mapped at higher elevations. The maximum precipitation in the Karakoram Range mostly occurred in the elevation zones higher than 3500 m (Hewitt et al. 1986). Estimations of the precipitation rates in this region also differed

widely from one observation to another (Palazzi et al. 2013). Other possible reasons may be systematic errors in precipitation gauging due to wind (Sevruk et al. 1989).

4 Conclusion

Snow-covered area change was monitored for glaciers with different aspects in three different seasons during the period 1990-2014. The glaciers are located around the main stream of the Indus River in northern Pakistan. The aim of this research was to map the seasonal snow-covered area of selected glaciers during the study period and to find a suitable image classification method to separate the snow-covered area from other land covers. The findings of the research can be summarized as follows:

The supervised image classification method is time consuming but relatively effective and provides more consistent results than the knowledge-based image classification method in terms of detecting glacier changes. Accuracy assessment of classified images showed 92% and 85% overall accuracy for the supervised and knowledge-based methods, respectively.

Seasonal snow-covered area maps of the early and late periods showed that the greatest snow-covered area was lost during the pre-monsoon season. The cause of the increased snow area reduction in the pre-monsoon season was due to the relatively large surface temperature difference between the early pre-monsoon and late pre-monsoon periods. During the early pre-monsoon season, the amount of fresh snow was largest and then gradually decreased in the late pre-monsoon season. Fresh snow has a maximum albedo, whereas aged snow has a relatively lower albedo and absorbs more solar radiation, thereby accelerating melting and snow-covered area reduction. Therefore, in the late pre-monsoon season, aged snow absorbed more solar radiation, leading to rapid melting. Similarly, a minimal snow-covered area was reduced during the monsoon season due to the low surface

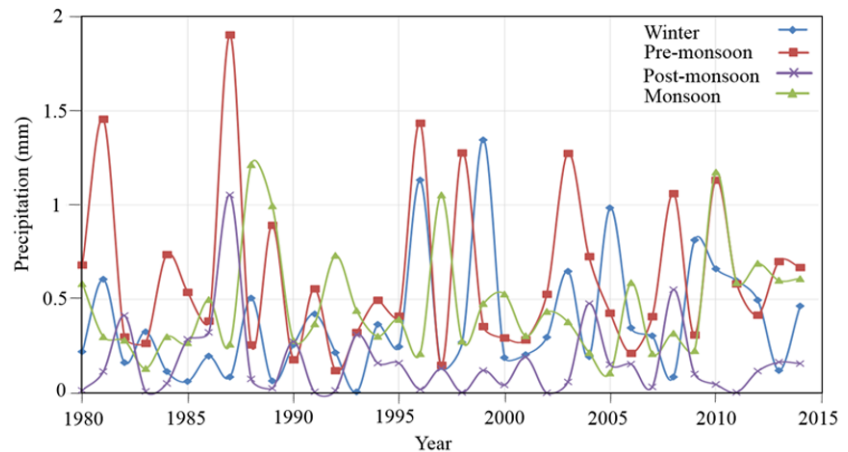


Figure 11 Seasonal average of daily precipitation during four seasons.

temperature difference between the early and late period monsoon. Therefore, it can be concluded that the greatest reduction in snow-covered area occurred in the pre-monsoon seasons and the lowest snow-covered areal reduction occurred in the monsoon seasons.

The glaciers facing east, north and south lost the most snow-covered area during the pre-monsoon season, and the glacier facing west lost the least snow-covered area during this season. Passu glacier (facing east) lost the largest amount of snow-covered area in the pre-monsoon season during the study period. In the monsoon season, Kunyang glacier (facing south) was advancing, and the other three glaciers, facing north, east and west, showed slight decreases in snow-covered area. Similarly, Passu glacier showed greater snow area reduction than Momhil glacier during the pre-monsoon season, but during the monsoon and post-monsoon seasons, Momhil glacier lost more snow area than Passu glacier. The melt rates of snow-covered area on the selected glaciers were different in the same season due to differences in aspect because the four glaciers were exposed to the same environmental conditions.

The snow-covered area maps for the early and late pre-monsoon season indicated that the snow-covered area was melted from the terminus of the glacier, that is, the low elevation (ablation) zones, mainly due to the relatively high glacier surface temperature at the terminus. The presence of debris near the terminus reduced the albedo, resulting in accelerated melting due to greater absorption of solar radiation. The snow-covered area in the accumulation zones was relatively

constant throughout the study period due the low surface temperature. Precipitation in the form of snow also increased the albedo and reduced the melting rate at the high-elevation zones.

The average daily maximum and daily mean temperatures in the winter and pre-monsoon seasons showed an increasing trend during the study period. Satellite-derived glacier surface temperature also showed an increasing trend during all seasons of the study period. Similarly, the negative correlation between seasonal mean temperature and seasonal snow-covered area indicated that the snow-covered area reduction was mainly due to increasing temperature. Past research has shown that snow-covered area was increasing in this region and global warming was not affecting glaciers located at high altitudes (Tahir et al. 2011); however, in our study, snow-covered area was decreasing on selected glaciers in all seasons except

winter. Therefore, it can be concluded that the decrease in snow-covered area may mainly be due to climate warming in the region.

Acknowledgments

This work was funded by National Natural Science Foundation of China (41421061, 41630754), Chinese Academy of Sciences (KJZD-EW-Go3-04), the State Key Laboratory of Cryospheric Science (SKLCS-ZZ-2017). We thank to the Pakistan Meteorological Department and the Water and Power Development Authority for contributing meteorological data. The authors also wish to thank United State Geological Survey (USGS) for providing Landsat images. Thanks to anonymous reviewers for their valuable and honorable comments.

References

- Albert TH (2002) Evaluation of remote sensing techniques for ice-area classification applied to the tropical Quelccaya Ice Cap, Peru. *Polar Geography* 26: 210-226. <https://doi.org/10.1080/789610193>
- Ali S, Dan L, Fu CB, Khan F (2015) Twenty first century climatic and hydrological changes over Upper Indus Basin of Himalayan region of Pakistan *Environ Res Lett* 10(1). <https://doi.org/10.1088/1748-9326/10/1/014007>
- Archer D (2003) Contrasting hydrological regimes in the upper Indus Basin. *Journal of Hydrology* 274: 198-210. [https://doi.org/10.1016/S0022-1694\(02\)00414-6](https://doi.org/10.1016/S0022-1694(02)00414-6)
- Barros AP, Chiao S, Lang TJ, et al. (2006) From weather to climate-Seasonal and interannual variability of storms and implications for erosion processes in the Himalaya. *Geological-Society-of-America Penrose Conference* 398: 17-38. [https://doi.org/10.1130/2006.2398\(02\)](https://doi.org/10.1130/2006.2398(02))
- Bhutiyan MR, Kale VS, Pawar NJ (2007) Long-term trends in maximum, minimum and mean annual air temperatures across the Northwestern Himalaya during the twentieth century *Climatic Change* 85: 159-177. <https://doi.org/10.1007/s10584-006-9196-1>
- Bolch T, Kulkarni A, Kääb A, et al. (2012) The State and Fate of Himalayan Glaciers. *Science* 336(6079): 310-314. <https://doi.org/10.1126/science.1215828>
- Bolch T, Menounos B, Wheate R (2010) Landsat-based inventory of glaciers in western Canada, 1985-2005. *Remote Sens Environ* 114(1): 127-137. <https://doi.org/10.1016/j.rse.2009.08.015>
- Bradley RS, Vuille M, Diaz HF, Vergara W (2006) Threats to water supplies in the tropical Andes. *Science* 312: 1755-1756. <https://doi.org/10.1126/science.1128087>
- Dankers R, De Jong SM (2004) Monitoring snow-cover dynamics in Northern Fennoscandia with SPOT VEGETATION images. *International Journal of Remote Sensing* 25: 2933-2949. <https://doi.org/10.1080/01431160310001618374>
- Dery SJ, Brown RD (2007) Recent Northern Hemisphere snow cover extent trends and implications for the snow-albedo feedback. *Geophysical Research Letter* 34(L22504). <https://doi.org/Artn L22504 10.1029/2007gl031474>
- Hewitt K (1985) The Upper Indus snow belts: SNOWFALL and sources of water yield. Snow and ice hydrology project: annual report: 58-63.
- IPCC (2007) Summary for policymakers. In: Solomon S, Qin D, Manning M, et al. (Eds.), *Climate Change 2007: The Physical Science Basis. Contribution of Working Group I to the Fourth Assessment Report of the Intergovernmental Panel on Climate Change*. Cambridge University Press, Cambridge, United Kingdom and New York, NY, USA
- IPCC (2013) Summary for Policymakers. In: *Climate Change 2013: The Physical Science Basis. Contribution of Working Group I to the Fifth Assessment Report of the Intergovernmental Panel on Climate Change* [Stocker TF, Qin D, Plattner GK, et al. (eds.)]. Cambridge University Press, Cambridge, United Kingdom and New York, NY, USA.
- Kaab A, Berthier E, Nuth C, et al. (2012) Contrasting patterns of early twenty-first-century glacier mass change in the Himalayas. *Nature* 488: 495-498. <https://doi.org/10.1038/nature11324>
- Kang S et al. (2015) Dramatic loss of glacier accumulation area on the Tibetan Plateau revealed by ice core tritium and mercury records. *Cryosphere* 9: 1213-1222. <https://doi.org/10.5194/tc-9-1213-2015>
- Kang SC, Xu YW, You QL, et al. (2010) Review of climate and cryospheric change in the Tibetan Plateau *Environ. Environmental Research Letters* 5(1). <https://doi.org/10.1088/1748-9326/5/1/015101>
- Kopacz M, Mauzerall DL, Wang J, et al. (2011) Origin and radiative forcing of black carbon transported to the Himalayas and Tibetan Plateau. *Atmos Chem Phys* 11: 2837-2852. <https://doi.org/10.5194/acp-11-2837-2011>
- Lau WKM, Kim KM (2012) The 2010 Pakistan Flood and Russian Heat Wave: Teleconnection of Hydrometeorological Extremes. *Journal of Hydrometeorol* 13: 392-403. <https://doi.org/10.1175/Jhm-D-11-016.1>
- Liang S, Fang H, Chen M (2001) Atmospheric correction of Landsat ETM+ Land surface Imagery: I. Methods. *IEEE Transactions on Geoscience and Remote Sensing* 39(11): 2490-2498. <https://doi.org/10.1109/36.964986>

- Maskey S, Uhlenbrook S, Ojha S (2011) An analysis of snow cover changes in the Himalayan region using MODIS snow products and in-situ temperature data. *Climatic Change* 108: 391-400. <https://doi.org/10.1007/s10584-011-0181-y>
- Menegoz M, Gallee H, Jacobi HW (2013) Precipitation and snow cover in the Himalaya: from reanalysis to regional climate simulations. *Hydrology and Earth System Sciences* 17(10): 3921-3936. <https://doi.org/10.5194/hess-17-3921-2013>
- Menegoz M, Krinner G, Balkanski Y, et al. (2013) Boreal and temperate snow cover variations induced by black carbon emissions in the middle of the 21st century. *Cryosphere* 7: 537-554. <https://doi.org/10.5194/tc-7-537-2013>
- Menegoz M et al. (2014) Snow cover sensitivity to black carbon deposition in the Himalayas: from atmospheric and ice core measurements to regional climate simulations. *Atmospheric Chemistry and Physics* 14(8): 4237-4249. <https://doi.org/10.5194/acp-14-4237-2014>
- Mooley D, Shukla J (1987) Variability and forecasting of the summer monsoon rainfall over India, in *Monsoon Meteorology*, C. P. Chang and T. N. Krishnamurti, Eds., Oxford University Press. pp 26-59.
- Muhammad S, Gul C, Javed A, et al. (2013) Comparison of glacier change detection using pixel based and object based classification techniques. *Geoscience and Remote Sensing Symposium (IGARSS) IEEE International*, 21-26 July 2013, pp. 4118-4121. <https://doi.org/10.1109/IGARSS.2013.6723739>
- Nagler T, Rott H, Malcher P, Muller F (2008) Assimilation of meteorological and remote sensing data for snowmelt runoff forecasting. *Remote Sens Environ* 112: 1408-1420. <https://doi.org/10.1016/j.rse.2007.07.006>
- Neckel N, Kropacek J, Bolch T, Hochschild V (2014) Glacier mass changes on the Tibetan Plateau 2003-2009 derived from ICESat laser altimetry measurements. *Environmental Research Letters* 9(1). <https://doi.org/10.1088/1748-9326/9/1/014009>
- Oerlemans J et al. (1998) Modelling the response of glaciers to climate warming. *Climate Dynamics* 14(4): 267-274. <https://doi.org/10.1007/s003820050222>
- Palazzi E, von Hardenberg J, Provenzale A (2013) Precipitation in the Hindu-Kush Karakoram Himalaya: Observations and future scenarios. *Journal of Geophysical Research Atmospheres* 118(1): 85-100. <https://doi.org/10.1029/2012JD018697>
- Paul F et al. (2013) On the accuracy of glacier outlines derived from remote-sensing data. *Annals of Glaciology* 54: 171-182. <https://doi.org/10.3189/2013AoG63A296>
- Paul F Kaab A, Maisch M, et al. (2004) Rapid disintegration of Alpine glaciers observed with satellite data. *Geophysical Research Letters* 31(21). <https://doi.org/10.1029/2004gl020816>
- Rees WG (2006) *Remote sensing of snow and ice*. Boca Raton, FL: CRC Press".
- Rabatel A et al. (2013) Current state of glaciers in the tropical Andes: a multi-century perspective on glacier evolution and climate change. *Cryosphere* 7: 81-102. <https://doi.org/10.5194/tc-7-81-2013>
- Racoviteanu AE, Arnaud Y, Williams MW, Ordonez J (2008) Decadal changes in glacier parameters in the Cordillera Blanca, Peru, derived from remote sensing. *Journal of glaciology* 54(186): 499-510. <https://doi.org/10.3189/002214308785836922>
- Rango A (1985) An International Perspective on Large-Scale Snow Studies. *Hydrological Sciences Journal* 30: 225-238. <https://doi.org/10.1080/02626668509490986>
- Rees WG (2006) *Remote sensing of snow and ice*. Boca Raton, FL: CRC Press.
- Sevruk et al. (1989) Reliability of Precipitation Measurement, International Workshop on Precipitation Measurement. WMO Tech. Document, pp 13-19.
- Sheikh MM, Manzoor N, Adnan, M, et al. (2009). *Climate Profile and Past Climate Changes in Pakistan*, GCISC-RR-01, Global Change Impact Studies Centre (GCISC), Islamabad, Pakistan, ISBN: 978-969-9395-04-8
- Shi YF, Liu SY (2000) Estimation on the response of glaciers in China to the global warming in the 21st century. *Chinese Science Bulletin* 45: 668-672. <https://doi.org/10.1007/Bf02886048>
- Sirguey P, Mathieu R, Arnaud Y, et al. (2008) Improving MODIS spatial resolution for snow mapping using wavelet fusion and ARSIS concept. *IEEE Geoscience and Remote Sensing Letters* 5: 78-82. <https://doi.org/10.1109/Lgrs.2007.908884>
- Stieglitz M, Ducharne A, Koster R, et al. (2001) The impact of detailed snow physics on the simulation of snow cover and subsurface thermodynamics at continental scales. *Journal of Hydrometeorology* 2(3): 228-242. [https://doi.org/10.1175/15257541\(2001\)002<0228:Tiodsp>2.0.Co;2](https://doi.org/10.1175/15257541(2001)002<0228:Tiodsp>2.0.Co;2)
- Tahir AA, Chevallier P, Arnaud Y, et al. (2011) Snow cover dynamics and hydrological regime of the Hunza River basin, Karakoram Range, Northern Pakistan. *Hydrology and Earth System Sciences* 15(7): 2275-2290. <https://doi.org/10.5194/hess-15-2275-2011>
- US EPA CCD Snow and Ice. <http://www3.epa.gov/climatechange/science/indicators/snow-ice/>, last updated: 11/11/2015.
- Williams Jr, RS, Hall DK, Sigurfsson O, et al. (1997) Comparison of satellite-derived with ground based measurements of the fluctuations of the margins of Vatnajökull, Iceland, 1973-1992. *Annals of Glaciology* 24: 72-80.
- Young GJ, Hewitt K (1990) Hydrology research in the Upper Indus Basin, Karakoram Himalaya, Pakistan, *Hydrology of Mountainous Areas, Czechoslovakia*, IAHS Publ 190: 139-152.
- Zhang GF, Li ZQ, Wang WB, Wang WD (2014) Rapid decrease of observed mass balance in the Urumqi Glacier No. 1, Tianshan Mountains, central Asia. *Quaternary International* 349: 135-141. <https://doi.org/10.1016/j.quaint.2013.08.035>